Molecular Biology of the Cell
Vol. 17, 723–737, February 2006

Biogenesis of Tubular ER-to-Golgi Transport Intermediates[V]

Jeremy C. Simpson,* Tommy Nilsson,† and Rainer Pepperkok*

*Cell Biology and Biophysics Programme, European Molecular Biology Laboratory, 69117 Heidelberg, Germany; and †Department of Medical Biochemistry, Göteborg University, 413 90 Gothenburg, Sweden

Submitted June 29, 2005; Revised November 8, 2005; Accepted November 16, 2005
Monitoring Editor: Benjamin Glick

Tubular transport intermediates (TTIs) have been described as one class of transport carriers in endoplasmic reticulum (ER)-to-Golgi transport. In contrast to vesicle budding and fusion, little is known about the molecular regulation of TTI synthesis, transport and fusion with target membranes. Here we have used in vivo imaging of various kinds of GFP-tagged proteins to start to address these questions. We demonstrate that under steady-state conditions TTIs represent ~20% of all moving transport carriers. They increase in number and length when more transport cargo becomes available at the donor membrane, which we induced by either temperature-related transport blocks or increased expression of the respective GFP-tagged transport markers. The formation and motility of TTIs is strongly dependent on the presence of intact microtubules. Microinjection of GTPγS increases the frequency of TTI synthesis and the length of these carriers. When Rab proteins are removed from membranes by microinjection of recombinant Rab-GDI, the synthesis of TTIs is completely blocked. Microinjection of the cytoplasmic tails of the p23 and p24 membrane proteins also abolishes formation of p24-containing TTIs. Our data suggest that TTIs are ER-to-Golgi transport intermediates that form preferentially when transport-competent cargo exists in excess at the donor membrane. We propose a model where the interaction of the cytoplasmic tails of membrane proteins with microtubules are key determinants for TTI synthesis and may also serve as a so far unappreciated model for aspects of transport carrier formation.

INTRODUCTION

Transport between adjacent membrane bound organelles in the secretory pathway is thought to be mediated by transport vesicles, which bud at the donor membrane and fuse at the acceptor membrane thereby delivering their cargo (reviewed by Lee *et al.,* 2004). Initially it was the use of biochemical assays that led to a basic understanding of this process (reviewed by Cook and Davidson, 2001) and the identification of many of the principal factors involved. However such approaches have revealed little about the physical nature and the dynamics of these carriers in the context of living cells.

Recent advances in light microscopy techniques, together with the availability of the green fluorescent protein (GFP; Chalfie *et al.,* 1994) and its spectral variants (reviewed by Zhang *et al.,* 2002), have enabled the in vivo study of membrane traffic events. Indeed nowhere have these technologies had greater impact than in visualizing traffic between the endoplasmic reticulum (ER) and Golgi complex (Presley *et al.,* 1997; Scales *et al.,* 1997). However, such experiments have also revealed that in addition to the presence of vesicular transport structures, in many instances secretory cargo can be seen in structures with a more tubular appearance. These tubular transport intermediates (TTIs) have been observed between the ER and the Golgi complex (Bannykh *et al.,* 1996; Blum *et al.,* 2000; Aridor *et al.,* 2001; Marra *et al.,* 2001; Mironov *et al.,* 2003), and in post-Golgi carriers (Hirschberg *et al.,* 1998; Toomre *et al.,* 1999; Polishchuk *et al.,* 2003). In all cases, because these TTIs have been seen to contain secretory cargo, it has been postulated that they are transport intermediates that may function alongside transport vesicles (reviewed by Kartberg *et al.,* 2005).

Although a vast amount of data are available on the molecular mechanisms that participate in the formation, transport, and fusion of vesicular carriers operating between the ER, the intermediate compartment (IC) and the Golgi (reviewed by Lee *et al.,* 2004), very little is known about the factors that regulate the biogenesis of tubular carriers. One reason for this is that these TTIs are very fragile and thus difficult to fix in cells, in turn making them difficult to study by immunocytochemistry, biochemistry, or electron microscopy, although recently attempts to characterize ER-to-Golgi intermediates at the ultrastructural level have been initiated (Horstmann *et al.,* 2002; Fan *et al.,* 2003). Detailed three-dimensional tomography and analysis of Golgi structure has also revealed the presence of tubular profiles in close proximity to the *cis* face of this organelle, although it is unclear as to what these structures actually are (Ladinsky *et al.,* 1999). Overall, little experimental data are available that address the question of whether these tubular carriers represent "normal" ER-to-Golgi transport for all cargo types. Indeed some data suggest that they represent alternative transport routes taken by specialized cargo (Stephens and Pepperkok,

This article was published online ahead of print in *MBC in Press* (http://www.molbiolcell.org/cgi/doi/10.1091/mbc.E05–06–0580) on November 28, 2005.

[V] The online version of this article contains supplemental material at *MBC Online* (http://www.molbiolcell.org).

Address correspondence to: Jeremy C. Simpson (simpson@embl.de) or Rainer Pepperkok (pepperko@embl.de).

Abbreviations used: BFA, brefeldin A; COP, coat protein; ER, endoplasmic reticulum; GDI, GTPase dissociation inhibitor; GFP, green fluorescent protein; IC, intermediate compartment; KDEL-R, KDEL receptor; TGN, *trans*-Golgi network; TTIs, tubular transport intermediates; VSV-G, vesicular stomatitis viral glycoprotein.

2002), whereas others propose that they are connectors of the late IC and the Golgi complex (Marra *et al.*, 2001).

The type of protein cargo present in TTIs is also an issue still to be resolved. Cargo can effectively be categorized into three classes, namely soluble, transmembrane, and large macromolecular, with each class presenting distinct needs to the cell's transport machinery. For example soluble and large macromolecular cargoes are unable to interact directly with the coat proteins (COPs) and other peripheral transport machinery located on the cytoplasmic face of the membrane, yet they can still signal their desire for transport. In addition, because of its size, macromolecular cargo will not fit into the 70–80-nm transport vesicles that have been classically described. Indeed in this case it is reasonable to suggest that suitable transport carriers will be tubular in appearance. Although the variety of cargo molecules studied has not been extensive, it is possible to find examples of each of these classes being present in tubular intermediates. A soluble form of GFP (Blum *et al.*, 2000) and the transmembrane lectin ERGIC-53 (Ben-Tekaya *et al.*, 2005) have both been seen in a tubulo-vesicular network between the ER and Golgi, and the large 300-nm cargo procollagen has also been visualized in tubular sacular structures (Bonfanti *et al.*, 1998; Mironov *et al.*, 2003; Trucco *et al.*, 2004). In the case of this latter study, the authors even provide evidence that it is the presence of this cargo that induces the formation of Golgi intercisternal tubules.

Tubular structures emanating from the Golgi complex have been studied for many years, and attempts have been made to modulate their formation. In this respect the fungal metabolite brefeldin A (BFA) has been one reagent that has been useful in understanding the relationship between coat protein complexes and tubule formation. Early studies demonstrated Golgi tubulation in BFA-treated (and indeed in untreated) cells and correlated these data with the loss of the β-COP subunit of the COPI coat protein from the membrane (Donaldson *et al.*, 1990; Cluett *et al.*, 1993). Similar BFA-induced tubules have also been visualized by GFP-tagging in living cells (Sciaky *et al.*, 1997). More recently incubation of cells at low temperatures (15°C) has also been shown to induce the presence of Golgi-derived tubules containing resident glycosylation enzymes (Martinez-Alonso *et al.*, 2005).

However, despite all this interest in tubules, we still have little understanding of what the factors are that most contribute to their formation and dynamics. In addition it is still unclear as to whether they represent bona fide ER-to-Golgi transport carriers and how much they contribute to the overall transport of cargo. Here we present detailed single cell analysis and quantification of TTIs containing various soluble and transmembrane cargoes in living cells and suggest a model for their biogenesis.

MATERIALS AND METHODS

Reagents

Expression constructs encoding GFP-KDEL-R and GFP-ERGIC-53 were kindly provided by Andrew Reynolds (Cancer Research UK) and David Stephens (University of Bristol, United Kingdom). In both cases the EGFP was inserted between the signal peptide and the mature protein. Soluble GFP has been previously described (Blum *et al.*, 2000). Nocodazole and GTPγS were from Calbiochem (Schwalbach, Germany), cycloheximide was from Sigma (St. Louis, MO), and rhodamine-labeled dextran and fluorescently-labeled secondary antibodies were from Molecular Probes (Leiden, The Netherlands). Synthetic peptides corresponding the tails of the p23 (hp24δ_1) and p24 (hp24β_1) proteins and a lumenal region of the p24 (hp24β_1) protein were synthesized and purified by Sigma Genosys (Cambridge, United Kingdom). Their sequences were CQVFYLRRFFKAKKLIE, CQIYYLKRFFEVRRVV, and CYKFCFSNRMSTMTPK, respectively. Peptides were dissolved in water at 2 mg/ml and stored at −20°C. The purification of Rab-GDI protein has been previously described (Horiuchi *et al.*, 1997). Antibodies used for immunofluorescence were against COPI coatomer (CM1A10; Palmer *et al.*, 1993), the β'-subunit of COPI (Pepperkok *et al.*, 1998), the γ-adaptin subunit of AP-1, GFP, GM130 (all BD Biosciences, Heidelberg, Germany), p27 (Fullekrug *et al.*, 1999), α-tubulin (Neomarkers, Fremont, CA), KDEL-R (Calbiochem), TGN46 (Serotec, Oxford, United Kingdom), and COPII (sec23; Affinity Bioreagents, Golden, CO). Antibodies against ERGIC-53 were a gift from H. P. Hauri (Basel, Switzerland). Antibodies against p24 have been previously described (Dominguez *et al.*, 1998).

The cell-line expressing p24 (hp24β_1) fused to EYFP was constructed in the following manner. Constructs encoding p23 (hp24δ_1) and p24 (hp24β_1) have been described previously (Blum *et al.*, 1999). The region coding for EGFP was replaced with ECFP or EYFP to produce p23-CFP and p24-YFP. HeLa cells were first transfected with p23-CFP and selected for stable expression using G418. Stable clones were assessed by light microscopy and screened for distinct juxta-nuclear Golgilike fluorescence. Some clones displayed juxta-nuclear but non-Golgilike staining, corresponding to proliferated ER as observed previously (Emery *et al.*, 2000). These clones were discarded. After clonal expansion, p23-CFP-expressing cells were retransfected with p24-YFP. This fusion protein was expressed from a puromycin-resistant plasmid. Cells were then selected for stable expression of both markers. After several passages, some cells developed into either p23-CFP or p24-YFP stable cells. Clones from the latter were used for this study.

Analysis of secretion in the p24-YFP cells was performed using recombinant adenoviruses encoding a CFP-tagged temperature-sensitive version of the vesicular stomatitis viral glycoprotein (VSV-G), ts045G. Detailed methodology has been previously described (Kerkhoff *et al.*, 2001).

Cell Culture

Vero (ATCC CCL-81) and HeLa cells (ATCC CCL-2) were routinely cultured in MEM and DMEM, respectively, supplemented with 10% fetal calf serum (FCS), glutamine, and penicillin/streptomycin. The p24-YFP HeLa stable cell line was maintained in DMEM/10% FCS, with the addition of 1 μg/ml puromycin (Sigma). Imaging was performed in glass-bottomed dishes (MatTek, Ashland, MA) in MEM medium lacking phenol red, FCS, and antibiotics, but containing 25 mM HEPES, pH 7.4.

Microinjection and Microscopy

Cells were microinjected using an Eppendorf microinjection system as previously described (Pepperkok *et al.*, 1993). Injection markers were used at a concentration of 0.4 mg/ml. Live cell microscopy was performed using a PerkinElmer Life and Analytical Sciences UltraView RS real-time confocal system (Boston, MA) consisting of a Zeiss Axiovert 200 microscope equipped with a 1.4 NA Plan Apo 60x objective (Jena, Germany). The system was contained within a perspex box allowing temperature control. Fixed cell images were acquired on a Leica TCS SP2 AOBS confocal laser rapid scanning microscope using a 1.4 NA PLAPO BL 63x objective, and using standard Leica software (Mannheim, Germany).

Experimental Setup

Vero cells were initially selected for the experiments with KDEL-R and ERGIC-53 because microinjection was facilitated by their larger size. Similar results were also obtained in HeLa cells however. All subsequent experiments were performed in HeLa cells because of their superior transfection efficiency. For analysis of soluble GFP transport, cells were transfected with the soluble GFP plasmid 18 h before the experiment as previously described (Simpson *et al.*, 2000). On the day of the experiment, the growth medium was exchanged for imaging medium and dishes were placed at 15°C for the lengths of time indicated. Cells were washed once with prewarmed (37°C) imaging medium, incubated at 37°C for 1 min in fresh imaging medium containing 100 μg/ml cycloheximide, before transfer to the microscope. Imaging was started within 3 min of the initial warming. For analysis of p24-YFP motility after the various treatments cells were incubated at 37°C for 10 min after microinjection to allow the cells to recover and then placed in imaging medium containing 100 μg/ml cycloheximide at 15°C for 30 min to accumulate cargo in the ERGIC compartment. The medium was then replaced with fresh imaging medium (37°C) also containing 100 μg/ml cycloheximide, and the dishes were directly transferred to the microscope. Imaging was started within 3 min of warming. All analyses were completed within 10 min of the original warming to 37°C.

Image Analysis and Quantification

All images were processed and quantified using NIH ImageJ version 1.33. Final movies were prepared using Apple QuickTime 6.5 (Apple Computer, Cupertino, CA) and were compressed using the Indeo Video 5.1 codec (Intel, Santa Clara, CA). Quantification of motility and fluorescence in cell populations was made from 100 to 150 cells for each experiment. Each experiment was performed at least twice. Cells were only considered to contain TTIs when two or more tubular structures per cell were observed by visual inspection of the videos within the duration of imaging (minimum 30 s). Structures were designated as "tubular" when their length was determined to

be greater than 2 μm at the level of light microscopy. Measurements were made using the line tool function of ImageJ. Other distinct punctate structures in the cell periphery were designated as "vesicular" when their length was below 2 μm. It should be noted that these latter structures are not necessarily the classically described 60–80-nm vesicles, because these would be below the resolution of detection by the methods used here. Motility of structures in individual cells was analyzed for a minimum of six cells for each experimental condition, and movies of 45-s duration were used. For quantification, images were thresholded and the number of structures were counted and the distance they moved during 45 s was determined using the ImageJ "Kymograph" macro. A detailed description of this macro can be found on the EAMNET website (http://www.embl.de/eamnet/html/downloads.html). Again, structures were only considered to be tubular when their length was greater than 2 μm. Western blots were quantified using Scion Image (Frederick, MD).

RESULTS

To have a greater understanding of the nature of transport carriers operating between the ER and Golgi complex, we decided to follow the spatial and temporal dynamics of various classes of cargo molecules that operate between these compartments in living cells. The KDEL receptor (KDEL-R) is one such example of a transmembrane protein that functions to retrieve soluble cargo containing an extreme C-terminal tetra-peptide motif "KDEL" from the Golgi back to the ER (Lewis and Pelham, 1990). In Vero cells microinjected with a construct encoding a GFP-tagged version of the KDEL-R (GFP-KDEL-R), using time-lapse microscopy it was possible to visualize a large number of punctate and highly motile structures moving between the juxtanuclear Golgi area and the cell periphery (Figure 1A and corresponding movie). However, in addition to the punctate carriers, in a number of the cells in the population it was also possible to observe motile structures that were distinctly tubular in appearance (Figure 1B, arrowheads, and corresponding movie). These tubular transport intermediates (TTIs) were variable in length, but most were also highly motile cycling in a manner similar to the punctate carriers. Surprisingly, the appearance of TTIs in cells was strongly dependent on the amount of plasmid DNA injected. Simply increasing the concentration of DNA resulted in an increase from 30 to 50% in the number of cells containing TTIs (Figure 1C). To see if this phenomenon was specific for this construct, we repeated these experiments but this time microinjecting a DNA encoding GFP-tagged ERGIC-53, another recycling protein of the ER-Golgi interface (Schindler *et al.*, 1993). Again it was possible to see TTIs in some cells of the population, although overall they were not as distinct as those seen with the KDEL-R (Figure 1D and corresponding movie). However, in a trend similar to that seen with the KDEL-R, microinjection of higher concentrations of the plasmid DNA also resulted in a greater frequency of cells containing TTIs after a fixed time period (unpublished data).

Because the amount of DNA available for transcription and translation appeared to have an effect on the presence of TTIs within cells, we next considered if expression time might also play a role. To this end we repeated the previous microinjection experiments but this time using a fixed concentration of DNA and adjusting the length of expression time. These experiments revealed a clear correlation between expression time and the frequency of TTIs in the population (Figure 1E). For the GFP-ERGIC-53 construct, although after 1 h of expression no cells containing TTIs could be detected, this proportion reached 20% after 5 h. In contrast, for GFP-KDEL-R, it was already possible to visualize TTIs in 12% of the cells after just 1 h, and this number increased to 35% after 5 h. Incubation times longer than this did not significantly increase the frequency of cells in the population containing TTIs (unpublished data). Together this suggests that either the availability of more DNA or greater expression times are factors contributing to the appearance of tubular ER-Golgi carriers. Both of these situations should result in cells producing a greater amount of protein, which in the case of both ERGIC-53 and the KDEL-R requires transport between the ER and Golgi. We therefore examined the time course experiments described above and quantified the mean fluorescence from individual cells either containing or not containing TTIs. In the case of the cells expressing GFP-KDEL-R, at all of the time points after microinjection those cells with TTIs showed an increased level of fluorescence compared with those cells without (Figure 1F). This was most striking at the longer expression times; for example, after 5 h, the cells without TTIs had on average only 40% of the fluorescence of the cells with TTIs. A similar, albeit less striking effect was also seen in the experiments with the GFP-ERGIC-53 construct. For example after 5 h of expression the cells without TTIs had on average 60% of the fluorescence of the cells with TTIs (Figure 1G). To validate our approach and to be certain that increased fluorescence correlated with an elevated amount of protein, we transfected Vero cells with the GFP-KDEL-R plasmid DNA and incubated them for increasing lengths of time. We were clearly able to identify a number of cells containing tubular structures, which was similar to the microinjection experiments. At each time point we visually determined the percentage of GFP-KDEL-R-expressing cells, quantified their mean fluorescence as before, and subjected equivalent numbers of transfected cells to SDS-PAGE and Western blotting with anti-GFP antibodies (Figure 1H). An increase in the amount of GFP-KDEL-R protein in the cells over time could clearly be detected by both analysis methods. We therefore attempted to correlate our fluorescence measurements with amounts of protein. For example in Figure 1F, the fluorescence measurements of cells containing TTIs indicated an increase in GFP-KDEL-R of ~5.5-fold over the time course. This would correspond to 4.8-fold if measured biochemically. This confirmed that our approach of using fluorescence to determine the relative increase in expressed protein yielded results similar to more conventional biochemical techniques.

To investigate whether the KDEL-R and ERGIC-53 TTIs that we had been analyzing with GFP-tagged proteins could also be observed with their endogenous counterparts in nonmanipulated Vero cells, we fixed and immunostained cells for these proteins. A number of ER-Golgi recycling proteins such as GRASP65 and indeed the KDEL-R have been previously reported to be present in tubular structures (Marra *et al.*, 2001). We were also able to detect a number of cells with this characteristic, which was similar to this earlier study (Figure 2), although the occurrence of such cells in the population was typically below 2%. Furthermore, unlike the situation seen with the GFP-tagged proteins in Figure 1, the number of these tubular structures per cell was also very low, with typically only one or two being visible in those cells in which they could be detected. Because we could not exclude the possibility that this low tubule abundance was due to poor preservation of these structures after fixation and the fact that this approach was unable to provide information about the dynamics of TTIs, we reverted to live cell experiments using fluorescently tagged reporters.

Because both KDEL-R and ERGIC-53 are transmembrane proteins, we next considered if TTI formation could also be observed and similarly modulated with a soluble cargo. Lumenal/soluble GFP is a previously described variant of GFP that contains a signal peptide in order to target the protein into the ER lumen, but because it contains no other

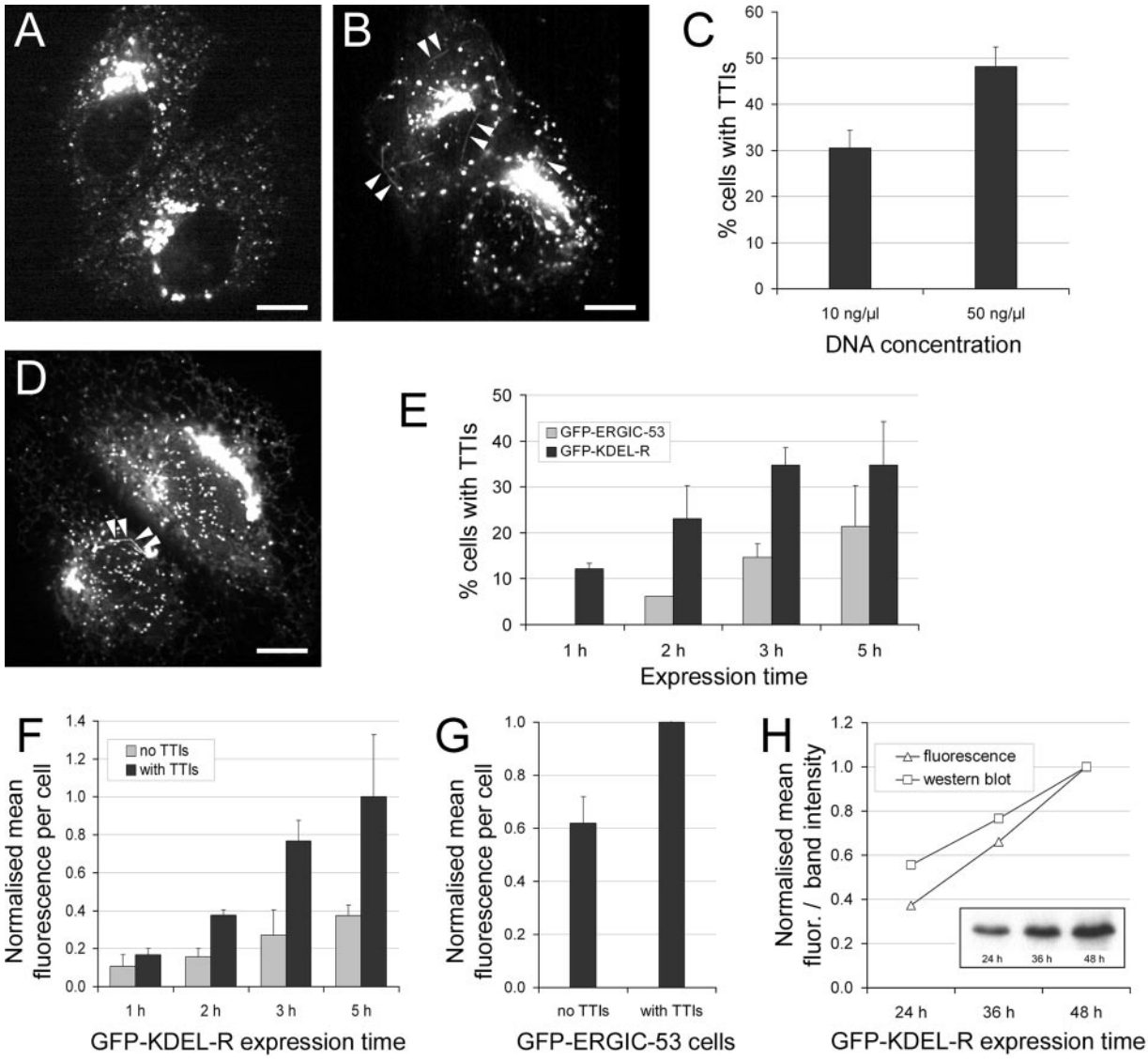

Figure 1. Expression levels of GFP-KDEL-R and GFP-ERGIC-53 influence TTI abundance. (A) Vero cell expressing low amounts GFP-KDEL-R showing the protein localizing to the Golgi and motile punctate structures. (B) Vero cell expressing a higher level of GFP-KDEL-R showing the protein also present in motile tubular carriers (arrowheads). (C) Vero cells were microinjected with two different concentrations of plasmid DNA encoding GFP-KDEL-R and incubated for 5 h. The frequency of cells in the population with distinct TTIs was determined. Error bars indicate mean and SD between duplicate experiments. (D) Vero cells expressing GFP-ERGIC-53 showing the protein predominantly present in vesicular structures, but also in motile tubular carriers (arrowheads) in some cells. (E) Vero cells were microinjected with 50 ng/μl plasmid DNA encoding either GFP-KDEL-R or GFP-ERGIC-53 and incubated for increasing lengths of time. The frequency of cells in the population with distinct TTIs was determined. (F) The mean GFP-KDEL-R fluorescence per cell was determined from the cells in E and plotted for cells containing (black bars) and not containing TTIs (gray bars). (G) The mean GFP-ERGIC-53 fluorescence per cell was determined from the cells in E after 5 h of expression. (H) Vero cells were transfected with plasmid DNA encoding GFP-KDEL-R and incubated for the times indicated. The mean fluorescence per cell was determined for each time point (triangles). In addition an equivalent number of transfected cells from each time point were lysed and subjected to SDS-PAGE and Western blotting with anti-GFP antibodies (see inset), and the amount of GFP-KDEL-R protein recovered was quantified (squares). Over the time course the mean values for the slopes were 1.355 (blot) and 1.511 (fluorescence). Error bars in E–G indicate mean and SD between duplicate experiments. Bars, 10 μm. Movies accompany A, B, and D.

targeting information, it is rapidly exported from the ER and is expelled from the cell via the classical secretory pathway (Blum *et al.*, 2000). To follow a wave of ER-to-Golgi transport of soluble GFP it was necessary to first incubate the cells at 15°C, in order to accumulate the newly synthesized cargo in the ERGIC compartment (Saraste and Kuismanen, 1984). On release of the temperature block, the soluble GFP was observed to travel rapidly toward the juxta-nuclear Golgi area of the cell, in most cases then appearing to fuse with existing structures at this location. Although these transport intermediates were highly pleiomorphic in size, within the population it was possible to find cells where the carriers were only punctate in shape (Figure 3A and corresponding movie) and other cells where TTIs were more prevalent (Figure 3B, arrowheads, and corresponding movie). We first decided to investigate the effect of holding the cells at 15°C

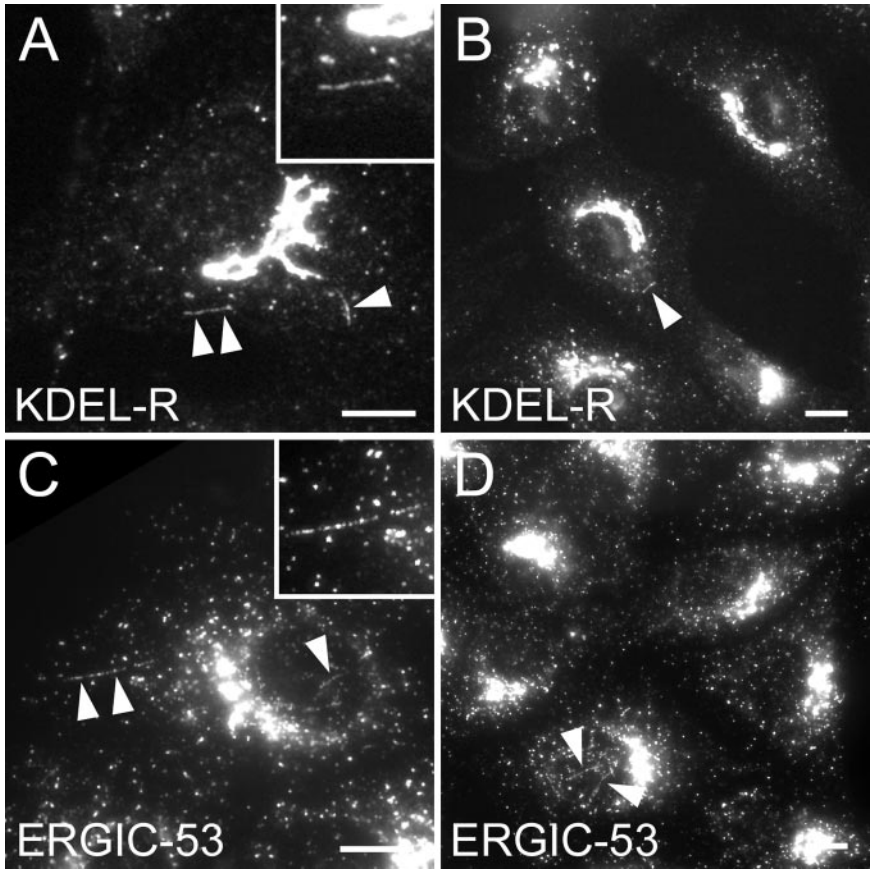

Figure 2. Visualization of endogenous TTIs. (A–D) Vero cells growing at 37°C were fixed and immunostained for endogenous KDEL-R (A and B) and ERGIC-53 (C and D). A small population of the cells contained visible tubular structures (arrowheads). Insets show enlargement of tubular structures marked with two arrowheads. Bars, 10 μm.

for increasing lengths of time and then after 5 min at 37°C determining the percentage of cells in the population containing TTIs. These experiments revealed that the length of the 15°C block had little effect on the overall frequency of TTI-containing cells within the population, with typically 60% of the cells having discernable tubular carriers (Figure 3C). We next considered the level of cargo expression in these cells compared with those cells lacking TTIs. We consistently found that cells with TTIs had on average 40% more expressed protein than those cells without TTIs, which was similar to the results obtained with the transmembrane proteins, but this was also irrespective of the time at 15°C (Figure 3D).

To understand in more detail the significance of TTIs with respect to transport, we examined the structures on an individual cell basis. Initially we counted the number of distinct punctate and tubular structures in cells that had been incubated at 15°C for either 1 or 5 h. We recorded that after 5 h of incubation, individual cells had 50% more soluble GFP-containing tubular structures than those cells only incubated for 1 h (Figure 3E), and in both cases 90% of these were motile (Figure 3F, black bars). In contrast, only about 40% of the punctate structures showed motility (Figure 3F, gray bars). When we considered only the motile structures in each cell, we found however that irrespective of incubation time, the TTIs only contributed to about 40% of the overall number of transport carriers (Figure 3G). Therefore although the longer incubation time resulted in a greater proportion of tubular structures in each cell, they were not per se contributing to an increase in transport of the cargo. What might therefore be the role of TTIs compared with punctate carriers? Finally we considered the average distance traveled by the two types of carrier. Reproducibly we found that the tubular carriers were moving 60% further than the punctate carriers, on average 13 μm compared with 8 μm in the fixed time intervals used in these experiments (see *Materials and Methods* for details; Figure 3H).

Further detailed analysis of soluble GFP transport carriers was difficult because of the short residence time of this cargo within the cell. Therefore we decided to focus on a recycling component of the early secretory pathway. The p24 family of proteins are small single transmembrane molecules that in living cells have been observed to recycle between the ER and Golgi complex (Blum *et al.*, 1999). Their precise function has not yet been elucidated, and although a role as putative cargo receptors between these compartments is one possibility (Muniz *et al.*, 2000), in yeast at least their presence is not essential for vesicular transport (Springer *et al.*, 2000). To work with a more homogeneous population of cells, we constructed a stable HeLa cell line expressing a YFP-tagged version of the p24 protein (see *Materials and Methods* for details). SDS-PAGE and Western blotting from these cells revealed the tagged protein to migrate at the expected molecular weight (Figure 4A). After quantifying the intensity of the p24 bands, and taking into account that only 18% of the cells in this population were actually expressing the tagged p24 protein, we determined the level of overexpression to be 3.5-fold over endogenous. Next we analyzed the subcellular localization of the p24-YFP protein using immunostaining with known markers of the endomembrane system. At 37°C the protein was found in a juxta-nuclear Golgi localization and in a number of distinct peripheral structures, overall displaying a similar distribution to that observed with the COPI coat complex (Figure 4B). This finding was in good

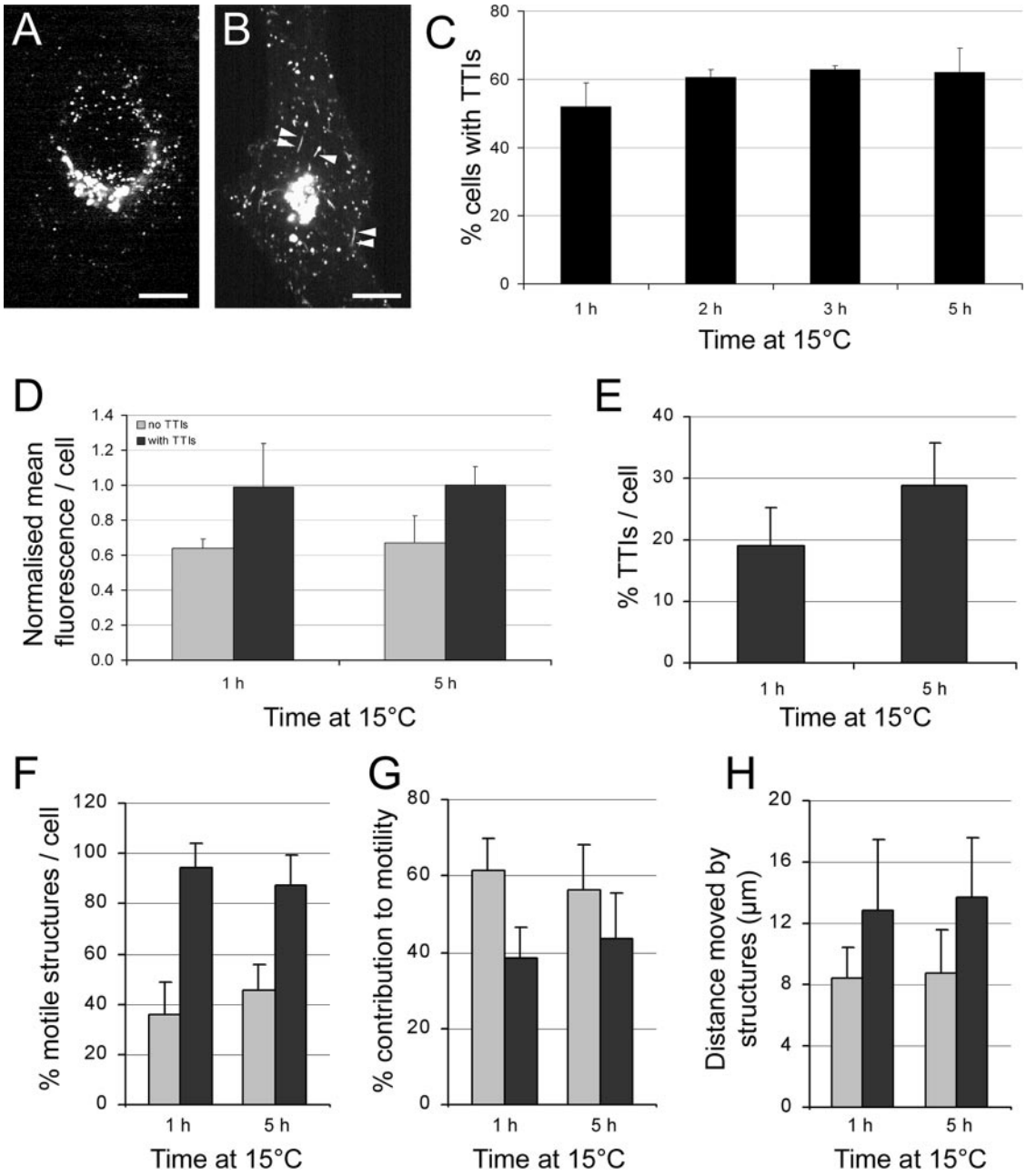

Figure 3. Soluble GFP cargo influences TTI abundance. (A and B) HeLa cells expressing soluble GFP after accumulation of the cargo at 15°C for 3 h followed by shifting the temperature to 37°C for 5 min. Some cells show transport of the cargo via vesicular carriers (A), other cells via TTIs (arrowheads; B). (C) HeLa cells expressing soluble GFP were incubated at 15°C for increasing lengths of time, followed by incubation at 37°C for 5 min. The frequency of cells in the population with distinct TTIs was determined. (D) The mean soluble GFP fluorescence per cell was determined from the cells in C from the 1- and 5-h time points and is plotted for cells containing (black bars) and not containing TTIs (gray bars). (E and F) Analysis of vesicular versus TTI carriers in individual cells incubated at 15°C for various lengths of time as indicated followed by incubation at 37°C for 5 min. Randomly selected distinct peripheral structures were counted and determined to be either vesicular or tubular. (E) The percentage of tubular structures at the various time points is shown. (F) The percentage of those structures that were motile is shown. Gray bars are vesicular carriers; black bars are tubular carriers. (G) Only motile structures were counted, and these were determined to be either vesicular or tubular, allowing their relative contribution to motility/transport to be determined. Gray bars are vesicular carriers; black bars are tubular carriers. (H) The distance moved by the motile structures was determined. Gray bars are vesicular carriers, black bars are tubular carriers. Error bars in C and D indicate mean and SD between duplicate experiments. Error bars in E–H indicate mean and SD between individual cells. Bars, 10 μm. Movies accompany A and B.

agreement with previous colocalization studies of these two proteins at the ultrastructural level (Lavoie *et al.*, 1999). In addition the p24-YFP protein also showed a good overlap in the Golgi area with p27, another member of the p24 family of proteins (Figure 4D), although few peripheral p27 structures were visualized with this antibody. A strong colocalization was also observed with endogenous KDEL-R and ERGIC-53, and a partial colocalization with the COPII sub-

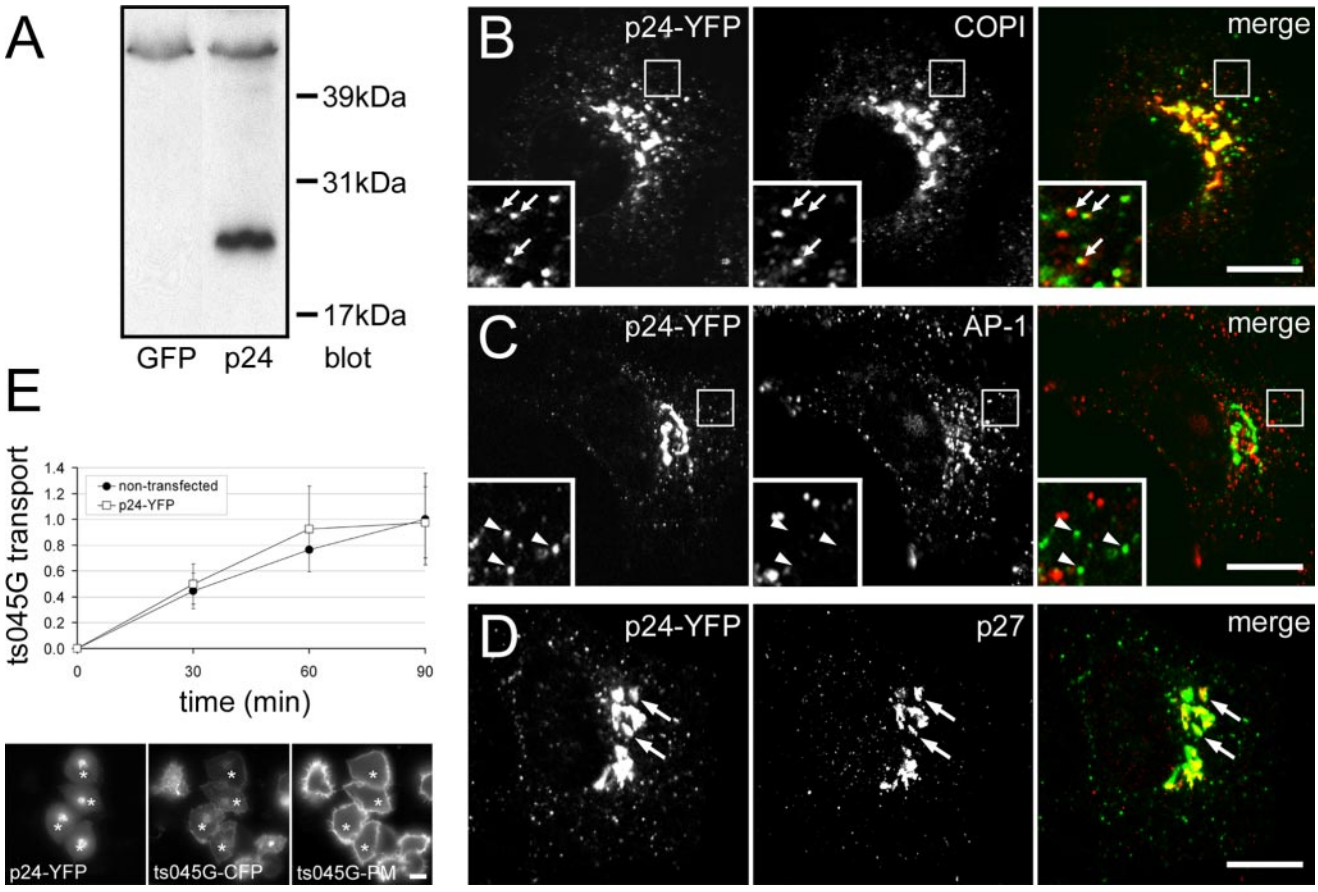

Figure 4. Characterization of a HeLa cell line stably expressing p24-YFP. (A) HeLa cells stably expressing p24-YFP were lysed and subjected to SDS-PAGE and Western blotting with either anti-GFP or anti-p24 antibodies. The blots revealed the presence of endogenous p24 protein and overexpressed p24-YFP at the anticipated sizes. In the population of cells used for Western analysis only 18% contained p24-YFP (unpublished data). Taken together with the quantification of the p24 and p24-YFP bands, a level of p24-YFP overexpression of 3.5-fold was determined. (B–D) HeLa p24-YFP cells were fixed and immunostained for the COPI coat complex (B), the AP-1 coat complex (C), and p27 protein (D). A high degree of colocalization of p24-YFP with COPI and p27, but not AP-1, was observed. (E) HeLa p24-YFP cells were subjected to a secretion assay using the temperature-sensitive variant (ts045G) of the VSV-G protein as a cargo marker. Little difference in the plasma membrane (PM) delivery of ts045G between p24-YFP expressing and nonexpressing cells was observed. Arrows in B–D indicate colocalizing structures, arrowheads designate noncolocalizing structures. Error bars in E indicate mean and SD between individual cells. Asterisks in E indicate p24-YFP expressing cells, with representative images from the 90-min time point. Bars, 10 μm.

unit sec23 (unpublished data). In contrast there was little overlap of p24-YFP with the *trans*-Golgi network (TGN) and endosomal coat complex AP-1 (Figure 4C), altogether indicating a correct distribution of p24-YFP in the early secretory pathway. Finally we assessed the functionality of these cells by performing a secretion assay using the temperature-sensitive variant (ts045G) of the vesicular stomatitis virus glycoprotein (VSV-G) as a cargo marker, and observing its arrival at the plasma membrane (Figure 4E). We were unable to detect any difference in the secretion rate of ts045G in the transfected compared with nontransfected cells in the population, suggesting that the presence of overexpressed p24-YFP was having little effect on normal membrane trafficking events as highlighted by ts045G.

In living cells the punctate p24-YFP structures were seen to be highly motile, continually moving between the cell periphery and the juxta-nuclear area (Figure 5A and corresponding movie). Again we looked in the population for cells containing tubular rather than vesicular carriers. At 37°C steady-state conditions, TTIs were detectable in only 18% of the cells, suggesting that transport was largely being mediated by carriers of a vesicular nature. Because p24 cycles via the ERGIC compartment we attempted to create an accumulation of p24-YFP cargo in this compartment using temperature blocks, as utilized in the experiments with soluble GFP. Such temperature treatments have previously been shown to cause a progressive accumulation of ERGIC-53 at this location (Klumperman *et al.*, 1998). We incubated cells for either 30 or 60 min at 15°C, then shifted them back to 37°C, and imaged them after a further 5 min. We observed a striking increase in the frequency of cells in the population now containing TTIs, compared with control conditions (Figure 5B, arrowheads, and corresponding movie). For example a 1-h arrest of transport in the ERGIC compartment, resulted in an increase of almost threefold in the number of cells now containing TTIs (Figure 5C). This increase in the prevalence of tubules was also visible within individual cells. Counting the distinct punctate and tubular structures revealed that under 37°C control conditions TTIs constituted only 10% of the total number of structures, whereas in the time immediately after release from the temperature blocks this proportion rose to 18% (Figure 5D). This increase in TTI abundance within individual cells returned to control levels after 30 min of incubation at 37°C, indicat-

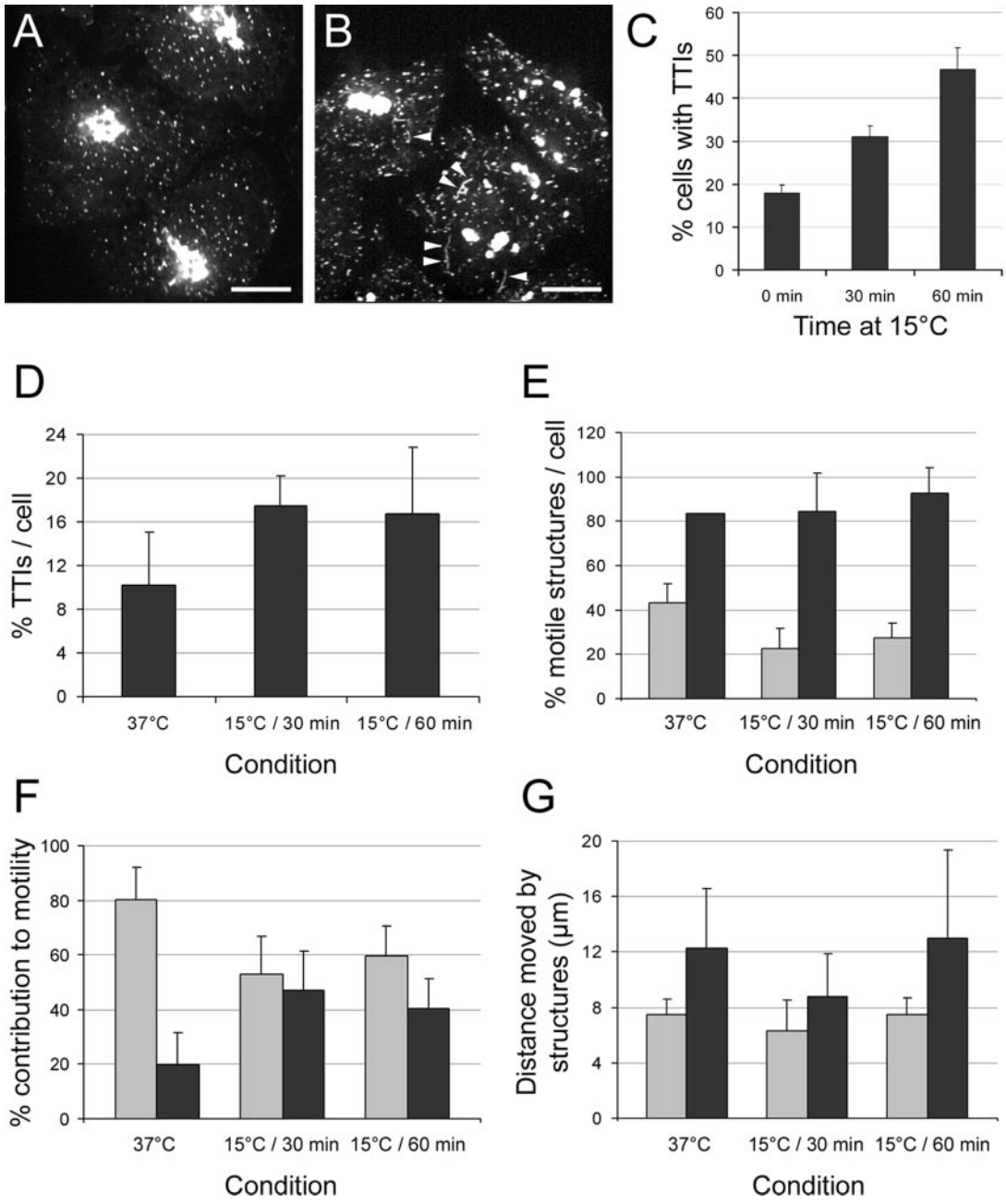

Figure 5. Release from temperature blocks enhances TTI formation. (A) HeLa cells stably expressing p24-YFP at 37°C. (B) HeLa cells stably expressing p24-YFP were incubated at 15°C for 30 min and then incubated at 37°C for 5 min. Tubular carriers become much more prominent (arrowheads). (C) HeLa cells stably expressing p24-YFP were either incubated at 37 or at 15°C for 30 or 60 min and then incubated at 37°C for 5 min. The frequency of cells in the population with distinct TTIs was determined. (D–G) Analysis of vesicular versus TTI carriers in individual cells incubated under the temperature regimes described above. Randomly selected distinct peripheral structures were counted and determined to be either vesicular or tubular. (D) The percentage of tubular structures under the various conditions is shown. (E) The percentage of those structures that were motile is shown. Gray bars are vesicular carriers; black bars are tubular carriers. (F) Only motile structures were counted, and these were determined to be either vesicular or tubular, allowing their relative contribution to motility/transport to be determined. Gray bars are vesicular carriers; black bars are tubular carriers. (G) The distance moved by the motile structures was determined. Gray bars are vesicular carriers; black bars are tubular carriers. Error bars in C indicate mean and SD between three replicate experiments. Error bars in D–G indicate mean and SD between individual cells. Bars, 10 μm. Movies accompany A and B.

ing that this was a transient response to the applied conditions (unpublished data). The actual length of the TTIs after the various temperature treatments remained constant however (Table 1).

We next examined the importance of the tubular carriers to transport. We noted that regardless of the conditions during the course of the experiment, on average 90% of the TTIs in the cells were moving, which was similar to the results with the soluble GFP cargo (Figure 5E, black bars). However when we calculated the contribution to motility made by all the moving carriers, we observed that after release from the temperature blocks the TTIs now accounted

Table 1. Quantification of TTI length in HeLa p24-YFP cells after various treatments

Treatment	TTI length ± SD (μm)
37°C	2.8 ± 0.8
15°C/30 min to 37°C	2.7 ± 0.5
15°C/60 min to 37°C	2.8 ± 0.3
15°C/30 min to 37°C (nocodazole)	3.3 ± 1.6
15°C/30 min to 37°C (washout)	3.7 ± 0.8
15°C/30 min to 37°C (GTPγS)	5.6 ± 0.8

for double (40%) the total number of moving structures compared with control conditions (Figure 5F). Finally we compared the distances moved by the two classes of transport intermediates. Although the various incubation conditions did not greatly affect the distances moved, we observed that some TTI structures often moved very large distances (up to 20 μm); however, because of the spread in this population the final average was not significantly different from that recorded for the vesicular carriers (Figure 5G).

The results above indicate that the enforced accumulation and subsequent release of transport-competent cargo from a donor membrane contributes to the formation of tubular carriers. Because the ultimate destination of these structures is most likely the same membranes as vesicular carriers, we were curious to determine whether similar transport machinery was utilized. Bi-directional transport between the ER and Golgi is known to involve the microtubule cytoskeleton. Disruption of this network using nocodazole has been shown by various studies to dramatically reduce both retrograde and anterograde transport between these membranes (Lippincott-Schwartz *et al.*, 1990; Scales *et al.*, 1997). Although these studies have proposed that microtubules only serve to increase the efficiency of transport, inevitably the reduced flow of material between these compartments is likely to result in a gradual accumulation of transport-competent cargo. Again we made use of the p24-YFP expressing cells for these experiments and used control conditions of a 30-min incubation at 15°C followed by a 5-min release at 37°C to reliably induce TTI formation. Initially we fixed the cells after this treatment to confirm that the microtubule cytoskeleton had indeed been depolymerized and that the overexpressed p24-YFP protein was not interfering with this process (Figure 6A). In addition we also immunostained the cells for the *cis*-Golgi marker GM130, and the TGN marker TGN46, to verify that the Golgi complex was still intact (Figure 6B). Next we analyzed the motility of the p24-YFP containing structures in living cells. When nocodazole was included during the 30-min incubation at 15°C, and after warming the cells to 37°C, we still observed a number of tubular structures present (Figure 6C, arrowheads, and corresponding movie). However when these experiments were repeated, but the nocodazole washed out, these tubules became more prominent (Figure 6D, arrowheads, and corresponding movie). The average length of these TTIs was also increased compared with control conditions (Table 1). Within the population of cells we observed an increase in the frequency of cells containing TTIs from 30 to 45% in the presence of nocodazole and an even more dramatic increase to 75% after nocodazole removal (Figure 6E). Analysis of the cells 30 min after the nocodazole washout revealed control levels of TTIs in the population (unpublished data). Although nocodazole treatment resulted in more cells containing visible tubules, when we looked at the actual number of these in individual cells, we found that not only had the number decreased (from 18 to 8% of the total distinct structures in nocodazole-treated cells; Figure 6F), but also that very few were motile (Figure 6G). Although it might have been expected that the motility of all the transport structures be abolished by this treatment, our previous immunostainings for the microtubule cytoskeleton had revealed that a small number of very short microtubules were still present in the cells at this time (Figure 6A, inset and arrowheads). In these cells we were also able to observe that p24-YFP TTIs and vesicular elements colocalized with these microtubule remnants, making it likely that the residual motility we detected was taking place on these structures. The removal of nocodazole resulted in an increase in the presence of TTIs in individual cells (25% of all structures; Figure 6F), and the motility of these was similar to the control (Figure 6G). Similarly, TTI contribution to overall motility in the cells treated with nocodazole was almost not detectable (Figure 6H). Analysis of the distance traveled by TTIs in the presence of nocodazole also showed that on average they were unable to travel more than 2 μm (Figure 6I), consistent with the lengths of microtubule remnants that could be detected (Figure 6A).

Membrane traffic is known to depend on a variety of other factors that associate with the cytoplasmic face of transport carriers. These include the Rab family of small GTPases (reviewed in Deneka *et al.*, 2003), and the COPI and COPII coat complexes (reviewed in Barlowe, 2000). In addition the p24 proteins themselves are also implicated in the regulation of transport between the ER and Golgi (Lavoie *et al.*, 1999; Belden and Barlowe, 2001). To test the importance of these factors with respect to TTI formation and motility, we microinjected various agents that selectively interfere with these components in turn and then incubated the cells at 15°C and then 37°C as before in order to promote TTI formation. Initially we injected synthetic peptides representing the cytoplasmic tails of the p24 and p23 proteins. Their presence had a dramatic effect on both the abundance and motility of all the carriers in the cell (Figures 7, A and B, and corresponding movies). TTIs were hardly detectable in these cells (Figure 7F), and the few that were identified showed no motility (Figures 7, G–I, black bars). In addition the motility of the vesicular carriers was also dramatically reduced in these cells; for example, when the p24 tail peptides were injected, <5% of these structures showed any significant movement (Figure 7G). To confirm that this striking result was not a nonspecific effect of peptide microinjection into the cells, we designed a third peptide representing a portion of the lumenal domain of p24, but having a pI and length similar to the p24 tail peptide. In living cells microinjected with this peptide and treated with the same temperature regime as before, the motility of p24-YFP structures (both tubular and vesicular) was observed to be similar to control noninjected cells (Figure 7C). Detailed quantification of p24-YFP motility from these cells also revealed a profile comparable to control noninjected cells (Figures 7, F–I).

To test the importance of Rab proteins for TTI activity, we next injected purified Rab-GDI (GTPase dissociation inhibitor) protein. Rab-GDI normally functions in the cytoplasm and holds Rab proteins in a soluble, inactive state, before their delivery to the membrane. Cells injected with Rab-GDI contained only a very small number of tubular structures (Figure 7D and corresponding movie, and Figure 7F), and we were unable to detect any motile TTIs in these cells (Figures 7G-I, black bars), which was similar to the experiments with the p23 and p24 peptides . Finally we injected cells with the poorly hydrolysable analogue of GTP, GTPγS.

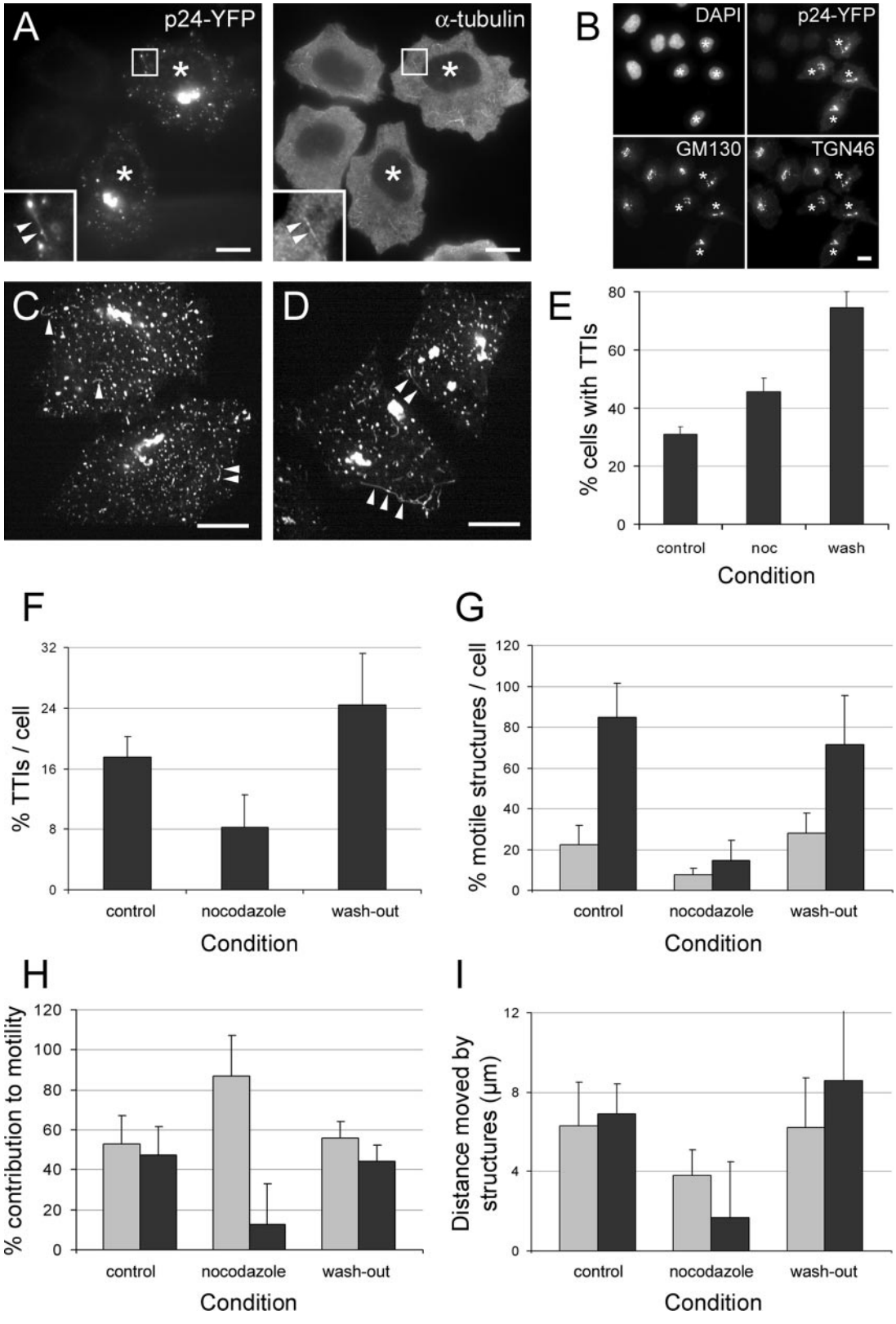
A
p24-YFP
α-tubulin
B
DAPI
p24-YFP
GM130
TGN46
C
D
E
% cells with TTIs
control
noc
wash
Condition
F
% TTIs / cell
control
nocodazole
wash-out
Condition
G
% motile structures / cell
control
nocodazole
wash-out
Condition
H
% contribution to motility
control
nocodazole
wash-out
Condition
I
Distance moved by structures (μm)
control
nocodazole
wash-out
Condition

Figure 6.

GTPγS has the effect of locking coat complexes on to transport-competent structures. On inspection of cells injected with GTPγS, we observed a large reticular network of tubular structures (Figure 7E, arrowheads, and corresponding movie). The frequency of these tubules within cells was much greater than in control cells (Figure 7F), and they were still contributing to the overall transport observed in the cells (Figures 7, G–I, black bars). However despite this treatment appearing to have the smallest effect with respect to motility, the tubules generated in these cells were the most dramatic, with their mean length increasing from 2.7 to 5.6 μm (Table 1).

From all the reagents used to try and modulate the formation of TTIs, the peptide tails of the p23 and p24 proteins proved to be most effective. Because transport between the ER and Golgi complex is highly dependent on the activity of the COPI and COPII coat complexes, we decided to visualize these coats in cells injected with these peptides. To our surprise we observed that despite the lack of both vesicular and tubular motility in these cells, both coats appeared to have a relatively normal appearance, being largely present on distinct membrane structures. Similar observations were made in cells injected with both the p23 (Figure 8A) and p24 tail peptides (Figure 8B).

DISCUSSION

Bi-directional transport of cargo and machinery molecules between the ER and Golgi complex is an essential cellular function. Using a variety of GFP-tagged marker proteins in living cells, we have observed that transport carriers operating at this interface can be both vesicular and tubular in appearance. Moreover we have shown here that the abundance of tubular carriers, both within a population of cells and in individual cells themselves, can be dramatically increased compared with steady state conditions. Here we have attempted to enforce the accumulation of cargo at donor membranes through the use of temperature blocks or the temporary removal of an intact microtubule cytoskeleton, and on release we observed a rapid proliferation of tubular carriers. In some instances these TTIs accounted for almost half of the motile transport carriers present in the cell.

However the treatments used here to enhance TTI production might be considered nonphysiological. In other words, the structures we have been observing could simply be an outcome of the cell being unable to manage an overload of ectopically expressed protein. As a consequence, excess cargo could result in a "swamping" of the conventional coat machinery necessary for vesicular carrier formation. Although this possibility cannot be excluded, and indeed here we have been obliged to work with ectopically expressed fluorescently tagged proteins in order to visualize and quantify their dynamics in living cells, a number of observations suggest that tubular structures may be genuine transport intermediates. First, and most importantly, we have been able to see them in nonperturbed cells, albeit in only a small percentage of the population (<2%). One possibility therefore is that the fixation methods utilized before immunostaining are inefficient in terms of TTI preservation. Using GFP-tagged constructs, we also were able to observe TTIs with soluble, transmembrane and recycling proteins, and in all cases they appeared to act as long-range carriers, not simply static entities linking membrane sites. Indeed in many instances, at least at the level of the light microscope, we were able to observe their appearance at potential donor membranes and disappearance into acceptor membranes. In addition, they are also likely to be transporting biologically useful material, because not only was their appearance transient, but their induction was very rapid such that they were unlikely to contain fluorescent protein aggregates. Quantifying the fluorescence in cells containing tubular carriers showed that these cells were expressing more of the transport marker than those in which tubules could not be detected. Altogether these data suggest that the increased presence of transport-competent cargo, compared with steady-state, can act as a trigger for TTI formation. It should also be noted however that the overall abundance of TTIs in nonperturbed cells (both in individual cells and in populations of cells) compared with vesicular carriers is very low. This may suggest that they participate in "on demand" specialized transport events such as those taken by cargo that is too large to be incorporated into 60–80-nm vesicles. A similar scenario has recently been proposed to explain the observation of small membrane continuities between Golgi cisternae (Marsh *et al.*, 2004; Trucco *et al.*, 2004), although the extent to which these are analogous structures to those we describe here still needs to be determined.

What might be the molecular mechanism underlying TTI biogenesis and movement? Vesicle and TTI formation are likely to share a similar contingent of core machinery molecules. For example, the ras-like small GTPases are essential for a variety of membrane traffic events, and indeed we observed here that the inhibition of Rab function by the presence of excess Rab-GDI protein almost totally abolished the synthesis and movement of both vesicular and tubular carriers. In stark contrast, the presence of GTPγS resulted in

Figure 6 (facing page). TTI motility is dependent on an intact microtubule cytoskeleton. (A and B) HeLa p24-YFP cells were incubated at 15°C for 30 min and then at 37°C for 5 min in the presence of 10 μM nocodazole before fixing and immunostaining for either α-tubulin (A) or GM130 and TGN46 (B). Under these conditions the microtubule cytoskeleton was almost totally dispersed; however, the Golgi complex and TGN retained their juxtanuclear localization. Remnants of microtubules often colocalized with p24-YFP vesicular and tubular structures (inset in A, arrowheads). Asterisks indicate p24-YFP expressing cells. (C) HeLa cells stably expressing p24-YFP were incubated at 15°C for 30 min in the presence of 10 μM nocodazole and then incubated at 37°C for 5 min. Short nonmotile TTIs can be observed (arrowheads). (D) HeLa cells stably expressing p24-YFP were incubated at 15°C for 30 min in the presence of 10 μM nocodazole, and then the nocodazole washed out and the cells were incubated at 37°C for 5 min. Longer TTIs can now be observed (arrowheads). (E) HeLa cells stably expressing p24-YFP were incubated as described above, and the frequency of cells in the population with distinct TTIs was determined. Control cells were incubated at 15°C for 30 min, and then at 37°C for 5 min, all in the absence of nocodazole. (F–I) Analysis of vesicular versus TTI carriers in individual cells incubated under the nocodazole treatments described above. Randomly selected distinct peripheral structures were counted and determined to be either vesicular or tubular. (F) The percentage of tubular structures under the various conditions is shown. (G) The percentage of those structures that were motile is shown. Gray bars are vesicular carriers; black bars are tubular carriers. (H) Only motile structures were counted, and these were determined to be either vesicular or tubular, allowing their relative contribution to motility/transport to be determined. Gray bars are vesicular carriers; black bars are tubular carriers. (I) The distance moved by the motile structures was determined. Gray bars are vesicular carriers; black bars are tubular carriers. Error bars in E indicate mean and SD between three replicate experiments. Error bars in F–I indicate mean and SD between individual cells. Bars, 10 μm. Movies accompany C and D.

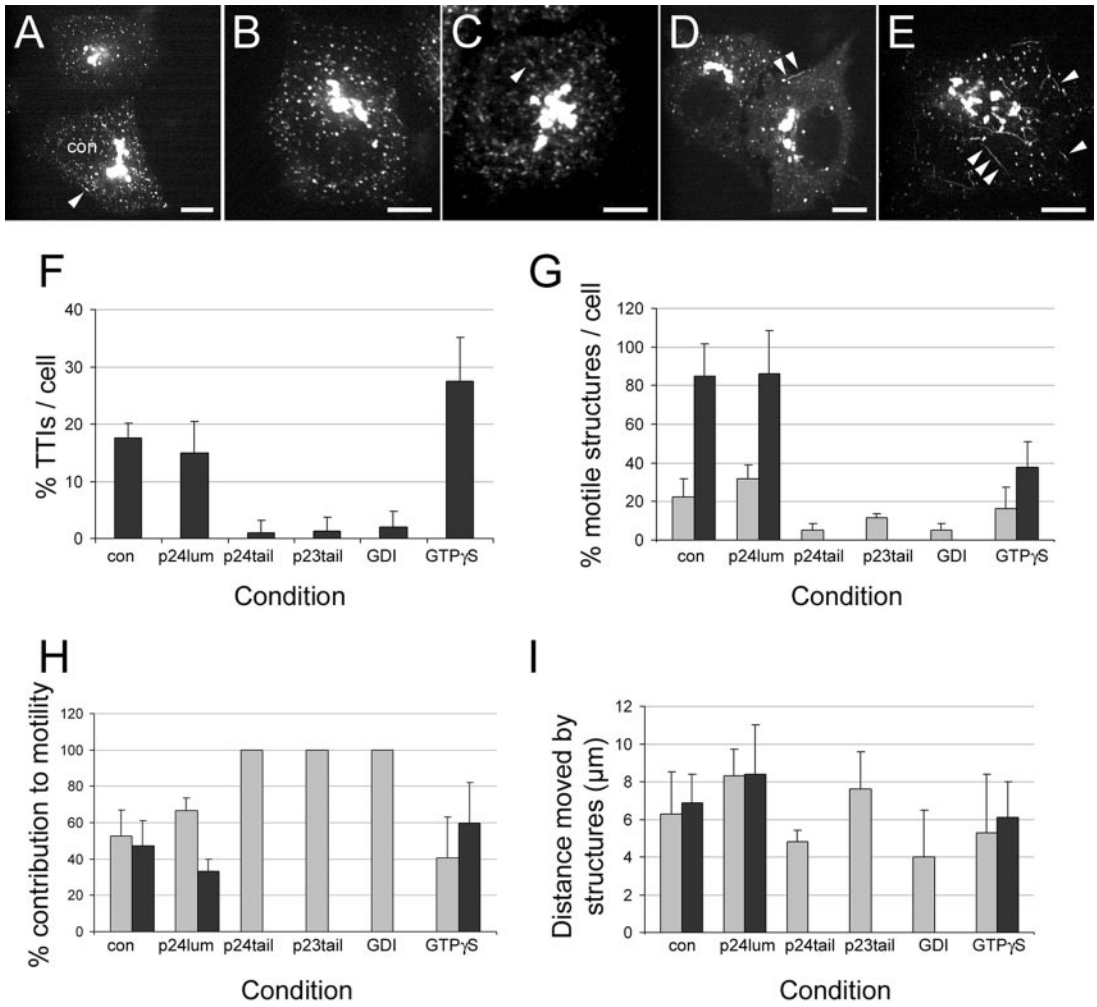

Figure 7. Regulation of TTIs involves other known membrane traffic components. (A–E) HeLa cells stably expressing p24-YFP after microinjection with various factors that may perturb membrane traffic. Example cells microinjected with 1 mg/ml p24 tail peptide (A), 1 mg/ml p23 tail peptide (B), 1 mg/ml p24 lumenal peptide (C), 0.5 mg/ml Rab-GDI (D), and 100 μM GTPγS (E) were incubated at 15°C for 30 min and then at 37°C for 5 min are shown. TTIs can be observed in some cells (arrowheads). A control noninjected cell is also shown in A (marked 'con'). (F–I) Analysis of vesicular versus TTI carriers in individual cells incubated under the various treatments described above. Randomly selected distinct peripheral structures were counted and determined to be either vesicular or tubular. (F) The percentage of tubular structures under the various conditions is shown. (G) The percentage of those structures that were motile is shown. Gray bars are vesicular carriers; black bars are tubular carriers. (H) Only motile structures were counted, and these were determined to be either vesicular or tubular, allowing their relative contribution to motility/transport to be determined. Gray bars are vesicular carriers; black bars are tubular carriers. (I) The distance moved by the motile structures was determined. Gray bars are vesicular carriers; black bars are tubular carriers. Error bars in F–I indicate mean and SD between individual cells. Bars, 10 μm. Movies accompany A–E.

the formation of an extensive tubular network that was often seen to link punctate elements. These tubules were largely immobile and did not readily detach from their donor membrane. Such nonhydrolyzable GTP analogues are known to prevent the release of vesicular coat proteins from membranes, a prerequisite for fusion of the carriers at the acceptor membrane. Similar to that described for vesicular carriers transporting VSV-G cargo between the ER and the Golgi (Pepperkok *et al.*, 1998), the formation of TTIs seems to be insensitive to GTPγS, but their fission and transport is inhibited. A more direct method to assess the importance of the vesicular coat in transport has been through the use of blocking antibodies that lock the coat on membranes (Pepperkok *et al.*, 1993). In these experiments secretory cargo was seen to be present in tubular structures that also contained ERGIC-53, but these were however mostly devoid of the COPI coat. Analysis of ERGIC-53-containing tubules generated in the presence of aluminum fluoride similarly showed a paucity of the COPI coat on these structures (Klumperman *et al.*, 1998). The common feature of all these experimental approaches is that they restrict the availability of coat to particular membranes. Under our experimental conditions it is conceivable that simply the presence of additional cargo overwhelms the coat machinery, thereby resulting in tubular rather than vesicular carriers. However the fact that under these conditions TTI formation actually appears to be promoted, is an indication that the coat per se might not be necessary for tubular carrier formation, but rather would have alternative roles. These might include enhancing the efficiency of carrier formation by assisting in the sorting and concentration of cargo at a predetermined site or linking the

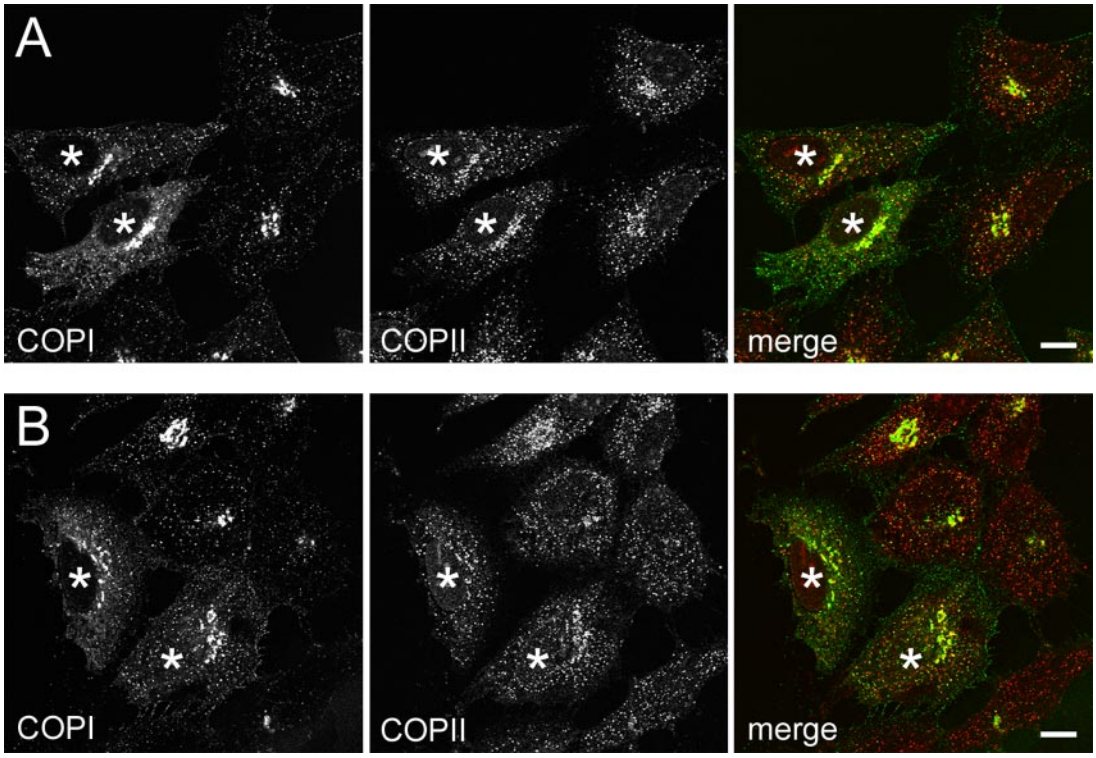

Figure 8. Peptide tails of p23 and p24 proteins do not affect COPI and COPII coat distribution. (A and B) Appearance of coat proteins in HeLa cells after microinjection with p23 or p24 peptide tails. HeLa cells were microinjected with 1 mg/ml p23 or p24 tail peptides and then incubated at 15°C for 30 min and then at 37°C for 5 min before fixing and immunostaining for COPI and COPII coat complexes. Cells in A were microinjected with p23 tail peptide, and cells in B with p24 tail peptide. Asterisks indicate injected cells. Bars, 10 μm.

membrane to additional cytoplasmic factors. Indeed at the ER, the sec24 subunit of the COPII coat has been shown to play a direct role in cargo selection (Miller *et al.*, 2002, 2003), and more recently the sec23 subunit to directly interact with the dynactin complex, thereby providing a link to the cytoskeleton (Watson *et al.*, 2005). Under conditions where either too little coat or an excess of transport-ready cargo was present at a particular membrane site, the outcome would still be the formation of a transport carrier, albeit one lacking the vesicular profile afforded by the presence of a rigid proteinaceous coat.

If such a mechanism were true, machinery to pull the transport carrier away from the donor membrane is still required. Work by Roux and colleagues (Roux *et al.*, 2002) potentially sheds light on how this may occur. They developed an experimental system whereby they could pull thin membrane tubes out of giant unilamellar vesicles and purified Golgi membranes. In this first study they also showed that the presence of kinesin motor proteins was essential for this process. In our work we show that an intact microtubule cytoskeleton is a key parameter for TTI biogenesis and subsequent motility in living cells. Furthermore, on restoration of this network after nocodazole treatment and washout, tubulation is greatly enhanced. This suggests that indeed motor proteins are key elements in TTI formation. Our preliminary unpublished data also suggest that one of these motors may be dynein, because microinjection of the p50/dynamitin dynactin subunit abolished p24-YFP TTI formation and movement.

However the question still remains as to how the cargo can influence TTI formation. Our experiments revealed that the simple accumulation of cargo was a strong factor in TTI synthesis. If cargo proteins were tightly sequestered in a small volume at a preferential site of transport, it is conceivable that they may change the local membrane environment. Different fluid domains in membranes have previously been shown to influence membrane curvature (Baumgart *et al.*, 2003; Roux *et al.*, 2005), and therefore a local high concentration of cargo protein would be a simple extension of this. Accumulating cargo would however still need to link with the microtubule network on the outer face of the membrane. This could most likely be achieved through the use of transmembrane proteins, because they can also act as bridges from soluble cargo inside the lumen of the donor membrane. Strikingly we observed a complete elimination of TTI synthesis when cells were injected with competing peptides representing the cytoplasmic tails of the p24 protein family. Yet despite this strong effect, the global appearance of the COPI and COPII coats in these cells remained unchanged at the peptide concentrations we used, excluding the possibility that the observed inhibitory effect of the tail peptides was solely caused by their removal of the membrane-associated coat. This raises the intriguing possibility that perhaps one function of the p24 proteins is to link transport-competent cargo with the cytoskeleton or motor proteins as the first step in TTI biogenesis. We are currently exploring this possibility.

Our results suggest a strong link between cargo accumulation and the formation of tubular carriers, leading to the hypothesis that TTIs are specialized carriers that could provide an additional mechanism to rapidly transport material between membranes. The further dissection of this machinery compared with that used in vesicle biogenesis will be the challenge ahead.

ACKNOWLEDGMENTS

We are grateful to Brigitte Joggerst and the EMBL Advanced Light Microscopy Facility (ALMF) staff for excellent technical support. We are also grateful to Birte Sönnichsen for providing the recombinant Rab-GDI protein, David Stephens for the GFP-ERGIC-53 construct, and Robert Blum and Irene Schultz for the p23 and p24 constructs. We also thank Eppendorf, Zeiss, PerkinElmer and Leica Microsystems for their continuous support of the EMBL ALMF.

REFERENCES

Aridor, M., Fish, K. N., Bannykh, S., Weissman, J., Roberts, T. H., Lippincott-Schwartz, J., and Balch, W. E. (2001). The Sar1 GTPase coordinates biosynthetic cargo selection with endoplasmic reticulum export site assembly. J. Cell Biol. *152*, 213–229.

Bannykh, S. I., Rowe, T., and Balch, W. E. (1996). The organization of endoplasmic reticulum export complexes. J. Cell Biol. *135*, 19–35.

Barlowe, C. (2000). Traffic COPs of the early secretory pathway. Traffic *1*, 371–377.

Baumgart, T., Hess, S. T., and Webb, W. W. (2003). Imaging coexisting fluid domains in biomembrane models coupling curvature and line tension. Nature *425*, 821–824.

Belden, W. J., and Barlowe, C. (2001). Distinct roles for the cytoplasmic tail sequences of Emp24p and Erv25p in transport between the endoplasmic reticulum and Golgi complex. J. Biol. Chem. *276*, 43040–43048.

Ben-Tekaya, H., Miura, K., Pepperkok, R., and Hauri, H. P. (2005). Live imaging of bidirectional traffic from the ERGIC. J. Cell Sci. *118*, 357–367.

Blum, R., Pfeiffer, F., Feick, P., Nastainczyk, W., Kohler, B., Schafer, K. H., and Schulz, I. (1999). Intracellular localization and in vivo trafficking of p24A and p23. J. Cell Sci. *112*, 537–548.

Blum, R., Stephens, D. J., and Schulz, I. (2000). Lumenal targeted GFP, used as a marker of soluble cargo, visualises rapid ERGIC to Golgi traffic by a tubulo-vesicular network. J. Cell Sci. *113*, 3151–3159.

Bonfanti, L. *et al.* (1998). Procollagen traverses the Golgi stack without leaving the lumen of cisternae: evidence for cisternal maturation. Cell *95*, 993–1003.

Chalfie, M., Tu, Y., Euskirchen, G., Ward, W. W., and Prasher, D. C. (1994). Green fluorescent protein as a marker for gene expression. Science *263*, 802–805.

Cluett, E. B., Wood, S. A., Banta, M., and Brown, W. J. (1993). Tubulation of Golgi membranes in vivo and in vitro in the absence of brefeldin A. J. Cell Biol. *120*, 15–24.

Cook, N. R., and Davidson, H. W. (2001). In vitro assays of vesicular transport. Traffic *2*, 19–25.

Deneka, M., Neeft, M., and van der Sluijs, P. (2003). Regulation of membrane transport by rab GTPases. Crit. Rev. Biochem. Mol. Biol. *38*, 121–142.

Dominguez, M., Dejgaard, K., Fullekrug, J., Dahan, S., Fazel, A., Paccaud, J. P., Thomas, D. Y., Bergeron, J.J.M., and Nilsson, T. (1998). gp25L/emp24/p24 protein family members of the *cis*-Golgi network bind both COP I and II coatomer. J. Cell Biol. *140*, 751–765.

Donaldson, J. G., Lippincott-Schwartz, J., Bloom, G. S., Kreis, T. E., and Klausner, R. D. (1990). Dissociation of a 110-kD peripheral membrane protein from the Golgi apparatus is an early event in brefeldin A action. J. Cell Biol. *111*, 2295–2306.

Emery, G., Rojo, M., and Gruenberg, J. (2000). Coupled transport of p24 family members. J. Cell Sci. *113*, 2507–2516.

Fan, J. Y., Roth, J., and Zuber, C. (2003). Ultrastructural analysis of transitional endoplasmic reticulum and pre-Golgi intermediates: a highway for cars and trucks. Histochem. Cell Biol. *120*, 455–463.

Fullekrug, J., Suganuma, T., Tang, B. L., Hong, W., Storrie, B., and Nilsson, T. (1999). Localization and recycling of gp27 (hp24gamma3): complex formation with other p24 family members. Mol. Biol. Cell *10*, 1939–1955.

Hirschberg, K., Miller, C. M., Ellenberg, J., Presley, J. F., Siggia, E. D., Phair, R. D., and Lippincott-Schwartz, J. (1998). Kinetic analysis of secretory protein traffic and characterization of golgi to plasma membrane transport intermediates in living cells. J. Cell Biol. *143*, 1485–1503.

Horiuchi, H., Lippe, R., McBride, H. M., Rubino, M., Woodman, P., Stenmark, H., Rybin, V., Wilm, M., Ashman, K., Mann, M., and Zerial, M. (1997). A. novel Rab5 GDP/GTP exchange factor complexed to Rabaptin-5 links nucleotide exchange to effector recruitment and function. Cell *90*, 1149–1159.

Horstmann, H., Ng, C. P., Tang, B. L., and Hong, W. (2002). Ultrastructural characterization of endoplasmic reticulum-Golgi transport containers (EGTC). J. Cell Sci. *115*, 4263–4273.

Kartberg, F., Elsner, M., Froderberg, L., Asp, L., and Nilsson, T. (2005). Commuting between Golgi cisternae—mind the GAP! Biochim. Biophys. Acta *1744*, 351–363.

Kerkhoff, E., Simpson, J. C., Leberfinger, C. B., Otto, I. M., Doerks, T., Bork, P., Rapp, U. R., Raabe, T., and Pepperkok, R. (2001). The Spir actin organizers are involved in vesicle transport processes. Curr. Biol. *11*, 1963–1968.

Klumperman, J., Schweizer, A., Clausen, H., Tang, B. L., Hong, W., Oorschot, V., and Hauri, H. P. (1998). The recycling pathway of protein ERGIC-53 and dynamics of ER-Golgi intermediate compartment. J. Cell Sci. *111*, 3411–3425.

Ladinsky, M. S., Mastronarde, D. N., McIntosh, J. R., Howell, K. E., and Staehelin, L. A. (1999). Golgi structure in three dimensions: functional insights from the normal rat kidney cell. J. Cell Biol. *144*, 1135–1149.

Lavoie, C., Paiement, J., Dominguez, M., Roy, L., Dahan, S., Gushue, J. N., and Bergeron, J. J. (1999). Roles for alpha(2)p24 and COPI in endoplasmic reticulum cargo exit site formation. J. Cell Biol. *146*, 285–299.

Lee, M. C., Miller, E. A., Goldberg, J., Orci, L., and Schekman, R. (2004). Bi-directional protein transport between the ER and Golgi. Annu. Rev. Cell Dev. Biol. *20*, 87–123.

Lewis, M. J., and Pelham, H. R. (1990). A human homologue of the yeast HDEL receptor. Nature *348*, 162–163.

Lippincott-Schwartz, J., Donaldson, J. G., Schweizer, A., Berger, E. G., Hauri, H. P., Yuan, L. C., and Klausner, R. D. (1990). Microtubule-dependent retrograde transport of proteins into the ER in the presence of brefeldin A suggests an ER recycling pathway. Cell *60*, 821–836.

Marra, P., Maffucci, T., Daniele, T., Tullio, G. D., Ikehara, Y., Chan, E. K., Luini, A., Beznoussenko, G., Mironov, A., and De Matteis, M. A. (2001). The GM130 and GRASP65 Golgi proteins cycle through and define a subdomain of the intermediate compartment. Nat. Cell Biol. *3*, 1101–1113.

Marsh, B. J., Volkmann, N., McIntosh, J. R., and Howell, K. E. (2004). Direct continuities between cisternae at different levels of the Golgi complex in glucose-stimulated mouse islet beta cells. Proc. Natl. Acad. Sci. USA *101*, 5565–5570.

Martinez-Alonso, E., Egea, G., Ballesta, J., and Martinez-Menarguez, J. A. (2005). Structure and dynamics of the Golgi complex at 15 degrees C: low temperature induces the formation of Golgi-derived tubules. Traffic *6*, 32–44.

Miller, E., Antonny, B., Hamamoto, S., and Schekman, R. (2002). Cargo selection into COPII vesicles is driven by the Sec24p subunit. EMBO J. *21*, 6105–6113.

Miller, E. A., Beilharz, T. H., Malkus, P. N., Lee, M. C., Hamamoto, S., Orci, L., and Schekman, R. (2003). Multiple cargo binding sites on the COPII subunit Sec24p ensure capture of diverse membrane proteins into transport vesicles. Cell *114*, 497–509.

Mironov, A. A. *et al.* (2003). ER-to-Golgi carriers arise through direct en bloc protrusion and multistage maturation of specialized ER exit domains. Dev. Cell *5*, 583–594.

Muniz, M., Nuoffer, C., Hauri, H. P., and Riezman, H. (2000). The Emp24 complex recruits a specific cargo molecule into endoplasmic reticulum-derived vesicles. J. Cell Biol. *148*, 925–930.

Palmer, D. J., Helms, J. B., Beckers, C. J., Orci, L., and Rothman, J. E. (1993). Binding of coatomer to Golgi membranes requires ADP-ribosylation factor. J. Biol. Chem. *268*, 12083–12089.

Pepperkok, R., Scheel, J., Horstmann, H., Hauri, H. P., Griffiths, G., and Kreis, T. E. (1993). Beta-COP is essential for biosynthetic membrane transport from the endoplasmic reticulum to the Golgi complex in vivo. Cell *74*, 71–82.

Pepperkok, R., Lowe, M., Burke, B., and Kreis, T. E. (1998). Three distinct steps in transport of vesicular stomatitis virus glycoprotein from the ER to the cell surface in vivo with differential sensitivities to GTP gamma S. J. Cell Sci. *111*, 1877–1888.

Polishchuk, E. V., Di Pentima, A., Luini, A., and Polishchuk, R. S. (2003). Mechanism of constitutive export from the golgi: bulk flow via the formation, protrusion, and en bloc cleavage of large trans-golgi network tubular domains. Mol. Biol. Cell *14*, 4470–4485.

Presley, J. F., Cole, N. B., Schroer, T. A., Hirschberg, K., Zaal, K. J., and Lippincott-Schwartz, J. (1997). ER-to-Golgi transport visualized in living cells. Nature *389*, 81–85.

Roux, A., Cappello, G., Cartaud, J., Prost, J., Goud, B., and Bassereau, P. (2002). A minimal system allowing tubulation with molecular motors pulling on giant liposomes. Proc. Natl. Acad. Sci. USA *99*, 5394–5399.

Roux, A., Cuvelier, D., Nassoy, P., Prost, J., Bassereau, P., and Goud, B. (2005). Role of curvature and phase transition in lipid sorting and fission of membrane tubules. EMBO J. *24*, 1537–1545.

Saraste, J., and Kuismanen, E. (1984). Pre- and post-Golgi vacuoles operate in the transport of Semliki Forest virus membrane glycoproteins to the cell surface. Cell *38*, 535–549.

Scales, S. J., Pepperkok, R., and Kreis, T. E. (1997). Visualization of ER-to-Golgi transport in living cells reveals a sequential mode of action for COPII and COPI. Cell *90*, 1137–1148.

Schindler, R., Itin, C., Zerial, M., Lottspeich, F., and Hauri, H. P. (1993). ERGIC-53, a membrane protein of the ER-Golgi intermediate compartment, carries an ER retention motif. Eur. J. Cell Biol. *61*, 1–9.

Simpson, J. C., Wellenreuther, R., Poustka, A., Pepperkok, R., and Wiemann, S. (2000). Systematic subcellular localization of novel proteins identified by large-scale cDNA sequencing. EMBO Rep. *1*, 287–292.

Springer, S., Chen, E., Duden, R., Marzioch, M., Rowley, A., Hamamoto, S., Merchant, S., and Schekman, R. (2000). The p24 proteins are not essential for vesicular transport in *Saccharomyces cerevisiae.* Proc. Natl. Acad. Sci. USA *97*, 4034–4039.

Sciaky, N., Presley, J., Smith, C., Zaal, K. J., Cole, N., Moreira, J. E., Terasaki, M., Siggia, E., and Lippincott-Schwartz, J. (1997). Golgi tubule traffic and the effects of brefeldin A visualized in living cells. J. Cell Biol. *139*, 1137–1155.

Stephens, D. J., and Pepperkok, R. (2002). Imaging of procollagen transport reveals COPI-dependent cargo sorting during ER-to-Golgi transport in mammalian cells. J. Cell Sci. *115*, 1149–1160.

Toomre, D., Keller, P., White, J., Olivo, J. C., and Simons, K. (1999). Dual-color visualization of trans-Golgi network to plasma membrane traffic along microtubules in living cells. J. Cell Sci. *112*, 21–33.

Trucco, A. *et al.* (2004). Secretory traffic triggers the formation of tubular continuities across Golgi sub-compartments. Nat. Cell Biol. *6*, 1071–1081.

Watson, P., Forster, R., Palmer, K. J., Pepperkok, R., and Stephens, D. J. (2005). Coupling of ER exit to microtubules through direct interaction of COPII with dynactin. Nat. Cell Biol. *7*, 48–55.

Zhang, J., Campbell, R. E., Ting, A. Y., and Tsien, R. Y. (2002). Creating new fluorescent probes for cell biology. Nat. Rev. Mol. Cell. Biol. *3*, 906–918.